

# Predictive Modeling and Optimization of Technological Response Parameters in Nd:YAG Laser Microgrooving of Titanium Alloy Using Combined RSM-PSO Approach



Samir Kumar Panda, Sudhansu Ranjan Das and Debabrata Dhupal

**Abstract** The present work focuses on modeling and optimization during Nd:YAG laser microgrooving of  $Ti_6Al_4V$  titanium alloy material with an objective to find the optimum process parameters settings for the groove upper width as well as depth and heat-affected zone. The experiments are performed as per Box–Behnken design of experiments (BBDOEs) with four process parameters (diode current, pulse frequency, scanning speed, and number of passes) for parametric optimization in order to control the technological response characteristics of the precision microgrooves on  $Ti_6Al_4V$  titanium alloy. Analysis of variance (ANOVA), response surface methodology (RSM) and particle swarm optimization (PSO) are subsequently proposed for predictive modeling and process optimization. The methodology described here is expected to be highly beneficial for manufacturing industries.

**Keywords** Laser microgrooving ·  $Ti_6Al_4V$  · ANOVA · RSM · PSO

## 1 Introduction

The recent technology has been advancing to infinite extent in search of newer materials and alloys with high hardness, strength and less weight which are very difficult to be machined with the conventional machining processes for achieving the required accuracy and precision. Nowadays, there is a vast demand for the well-finished products of titanium alloy materials with high accuracy and complex integrated designs. Such features on a component can be achieved only through the advanced manufacturing process, especially by laser beam machining. In case of micromachining the feature size is less than 1 mm. Hence lasers are increasingly employed for a precise micromachining because their beams can be focused accurately on microscopic areas, and attributed to a number of advantages which are normally applicable to whole range of the materials processing applications, like, non-contact processing,

---

S. K. Panda · S. R. Das (✉) · D. Dhupal  
Veer Surendra Sai University of Technology, Burla 768018, India  
e-mail: [das.sudhansu83@gmail.com](mailto:das.sudhansu83@gmail.com)

© Springer Nature Singapore Pte Ltd. 2020  
L. Vijayaraghavan et al. (eds.), *Emerging Trends in Mechanical Engineering*,  
Lecture Notes in Mechanical Engineering,  
[https://doi.org/10.1007/978-981-32-9931-3\\_17](https://doi.org/10.1007/978-981-32-9931-3_17)

high productivity, eradication of the finishing operations, minimized cost of processing, and enhanced the quality of product, maximize material utilization, green manufacturing and minimize the heat-affected zone. The above-cited advantages can only be obtained with appropriate selection of process parameters. Researchers have employed various methods MRA [1, 2] and ANN [3, 4] for mathematical modeling in order to predict the responses and Taguchi method [5], RSM [6, 7], GA [8, 9], PSO [10, 11] for optimization the controlled process parameters during laser micromachining process, that have been explored as productivity and reliable tool in advanced computing technology for high-quality frameworks since it gives a straight-forward, skilled, and systematically optimize the output, such as cost, quality, and performance. The proper utilization, along with appropriate adjustment of machining controllable process parameters are of main importance for achieving fine grade of microgrooves, which generally utilize proper time and effort due to the frequently changing behavior of the laser micromachining process. Thus, the present study focuses on development of mathematical models and multi-response parametric optimization during laser microgrooving of titanium alloy ( $Ti_6Al_4V$ ) through Nd:YAG laser treatment using statistical approach such as response surface methodology (RSM) followed by, computational approach like particle swarm optimization (PSO).

## 2 Experimental Procedure

A 75 W diode-pumped Nd:YAG laser (make: Sahajanand, model: SPRIGO LD) was used to conduct the experiments which has assist gas supply unit. During experiment, the laser beam (focal length of 77 mm) has been set at surface of the workpiece as the focal plane which resulted in laser beam spot size around 21  $\mu\text{m}$ . In the present research,  $Ti_6Al_4V$  titanium alloy plate of dimension (75 mm \* 25 mm \* 5 mm) is considered as the workpiece material for experimentation, subjected to microgrooving by multiple laser pulses (DPSS Nd:YAG laser treatment) with actual peak power vary between 0.7–5 kW.

In the current investigation diode current, pulse frequency, scan speed, and number of pass are considered as the input process parameters which influence the technological response characteristics of laser microgrooving such as, upper width, heat-affected zone and groove depth. The different process parameters and their values are shown in Table 1. Using the abovementioned process parameters (4) each with five different levels, a well-designed experimental layout is formulated in conformance with Box–Behnken design of experiments (BBDOEs) which is consisting of thirty-one (31) number of trials. Design of experimental plan with actual value of process parameters, measured response are presented in Table 2. All the experiential trials for laser engraving are performed with argon gas. The upper width (GWD), heat affected zone (HAZ) and groove depth (GD) of machined microgroove is measured by utilizing scanning electron microscope (make: Hitachi, model: SU3500).

**Table 1** Process parameters and levels

Parameters	Symbols	Units	Levels				
			-2	-1	0	1	2
Diode current	$X_1$	amp	18.5	20	21.5	23	24.5
Pulse frequency	$X_2$	kHz	28	31	34	37	40
Scan speed	$X_3$	mm/s	40	50	60	70	80
Number of passes	$X_4$		9	10	11	12	13

The schematic view of experimental work and methodology proposed in the current study, is presented in Fig. 1.

### 3 Results and Discussion

#### 3.1 Development of Response Model

The results of response characteristics, i.e., groove width (GWD), groove depth (GD) and heat-affected zone (HAZ) which were obtained in accordance of BBDOEs, were analyzed in Minitab 16 through response surface methodology (RSM) and developed the mathematical models to find-out the best-fit of correlation between the abovementioned response (GWD, GD, HAZ) of the microgrooved component with the input parameters such as diode current ( $X_1$ ), pulse frequency ( $X_2$ ), scanning speed ( $X_3$ ) and number of passes ( $X_4$ ). Regression equations in the second-order (i.e., quadratic model) for the responses are presented by:

$$\begin{aligned}
 Y_{GWD} = & -2663 + 37.6X_1 + 47.5X_2 - 1.29X_3 + 303.1X_4 + 2.199X_1^2 + 0.272X_2^2 \\
 & + 0.00573X_3^2 - 3.052X_4^2 - 1.458X_1X_2 - 0.1708X_1X_3 - 5.958X_1X_4 \\
 & + 0.0604X_2X_3 - 3.354X_2X_4 + 0.194X_3X_4
 \end{aligned} \tag{1}$$

$$\begin{aligned}
 Y_{HAZ} = & 1189 - 54X_1 - 2.93X_2 - 14.64X_3 - 15.2X_4 - 0.428X_1^2 \\
 & - 0.4888X_2^2 - 0.008X_3^2 - 1.4X_4^2 + 0.915X_1X_2 + 0.3287X_1X_3 \\
 & + 2.437X_1X_4 + 0.2694X_2X_3 - 0.073X_2X_4 - 0.0731X_3X_4
 \end{aligned} \tag{2}$$

$$\begin{aligned}
 Y_{GD} = & 2222 - 383.7X_1 + 166.7X_2 + 10.03X_3 - 238X_4 + 9.370X_1^2 \\
 & - 0.49X_2^2 - 0.1816X_3^2 + 20.09X_4^2 - 5.083X_1X_2 + 1.408X_1X_3 \\
 & + 7.58X_1X_4 + 0.521X_2X_3 - 4.71X_2X_4 - 3.088X_3X_4
 \end{aligned} \tag{3}$$

To avoid the misleading conclusion, statistical analysis is performed for the proposed RSM models (GUV, HAZ, and GD) by employing ANOVA in order to check

**Table 2** Design of experimental plan and experimental results

Run	Coded values				Actual settings				Responses			
	X <sub>1</sub>	X <sub>2</sub>	X <sub>3</sub>	X <sub>4</sub>	Diode current (amp)	Frequency (kHz)	Scan speed (mm/s)	No. of passes	G UW (μm)	HAZ (μm)	GD (μm)	
1	1	1	-1	-1	23	37	50	10	334.0938	48.865	244.989	
2	0	0	0	-2	21.5	34	60	9	277.406	62.684	378.406	
3	-1	-1	1	1	20	31	70	12	309.968	36.978	252.364	
4	-1	1	-1	-1	20	37	50	10	303	41.787	295.25	
5	0	0	0	0	21.5	34	60	11	305.5	62.314	323.75	
6	0	0	0	2	21.5	34	60	13	297.781	58.471	457.197	
7	0	-2	0	0	21.5	28	60	11	301.281	52.196	291.781	
8	-1	1	1	-1	20	37	70	10	304.343	47.865	395.177	
9	-1	1	1	1	20	37	70	12	315.75	37.362	331.666	
10	-1	-1	-1	-1	20	31	50	10	258.468	71.265	240.197	
11	0	0	0	0	21.5	34	60	11	299.25	66.764	335.5	
12	0	0	0	0	21.5	34	60	11	292.25	64.764	327	
13	2	0	0	0	24.5	34	60	11	335.281	74.184	452.197	
14	-1	-1	1	-1	20	31	70	10	256.875	47.225	272.562	
15	1	-1	-1	-1	23	31	50	10	320	68.037	264.375	
16	1	-1	-1	1	23	31	50	12	329.718	71.378	425.177	
17	0	0	0	0	21.5	34	60	11	301.25	65.939	334.75	
18	1	-1	1	-1	23	31	70	10	310.968	58.190	387.677	
19	0	0	2	0	21.5	34	80	11	301.156	56.196	311.822	
20	-1	1	-1	1	20	37	50	12	301.093	32.953	352.677	

(continued)

Table 2 (continued)

Run	Coded values				Actual settings				Responses			
	X <sub>1</sub>	X <sub>2</sub>	X <sub>3</sub>	X <sub>4</sub>	Diode current (amp)	Frequency (kHz)	Scan speed (mm/s)	No. of passes	GUV (µm)	HAZ (µm)	GD (µm)	
21	0	0	0	0	21.5	34	60	11	300.75	69.014	304.75	
22	-1	-1	-1	1	20	31	50	12	312.5	70.862	355.687	
23	0	0	0	0	21.5	34	60	11	304.75	64.264	304.875	
24	0	0	-2	0	21.5	34	40	11	303.031	69.759	217.781	
25	1	1	-1	1	23	37	50	12	301.875	59.875	338.479	
26	1	-1	1	1	23	31	70	12	319.75	66.512	424.791	
27	0	2	0	0	21.5	40	60	11	317.906	44.959	347.822	
28	1	1	1	1	23	37	70	12	306.593	80.378	393.156	
29	0	0	0	0	21.5	34	60	11	303.25	63.239	341.375	
30	1	1	1	-1	23	37	70	10	319.25	74.537	413.354	
31	-2	0	0	0	18.5	34	60	11	303.906	50.471	391.406	

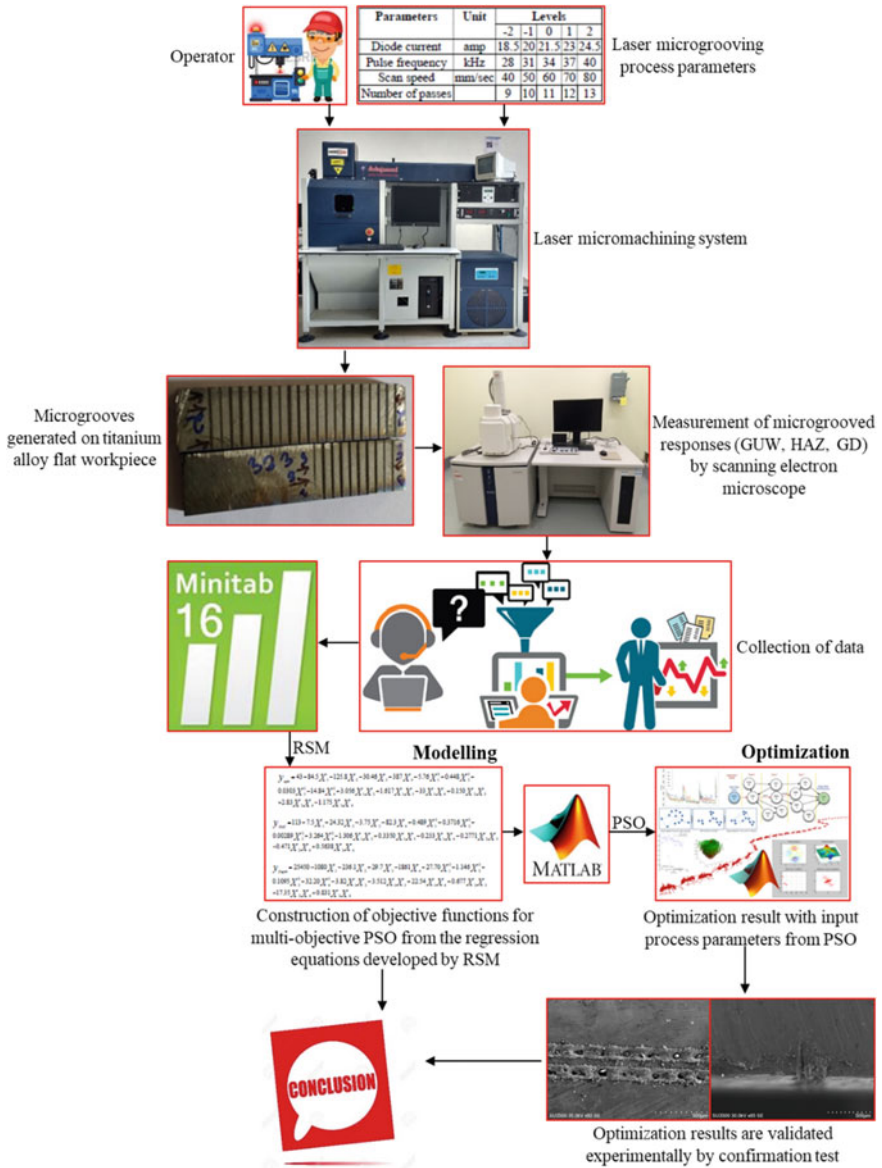


Fig. 1 Schematic layout of experimental setup and methodology proposed

their adequacy and validity, as shown in Table 3. The estimate  $F$ -value of the models for GUW, HAZ, and GD are 27.14, 25.15, and 31.05, respectively, which shows the excellent significance of model because of lower magnitude of  $F$ -table value (2.46) at 95% of confidence level. Moreover, it can be clearly seen that the developed quadratic models are statistically significant as the  $P$  (probability) value is under 0.05. Particularly, the model developed using RSM for groove width, groove depth and heat-affected zone explain the  $R^2$  values (i.e., co-efficient of determination) of 0.959, 0.956, and 0.964, respectively, which are very close to unity (1) ensuring the excellent fit for the model with greater statistical significance. Finally, normal probability plot combined with Anderson–Darling test for GUW, HAZ, and GD is shown in Fig. 2, which ensures that the residuals distributed fairly close to a straight line indicating that the errors are dispersed normally and specifying that the terms associated with the model are significant. With  $p$ -value (0.103 for GUW, 0.055 for HAZ, and 0.11 in case of GD) received from Anderson–Darling test is greater than significance level value (0.05), which confirms the adequacy of models as no reason was observed for the rejection of null-hypothesis. Hence, the proposed predictive can be utilized for particle swarm optimization.

### 3.2 Response Optimization Using PSO

Alternative method like GA, claimed to be more efficient for simultaneous optimization of multiple responses. However, the computational effort required by PSO to arrive to such high-quality solutions is less than the effort required to arrive at the same high-quality solutions by the GA, which pursuits us to consider PSO in the present study. PSO is a soft computing approach which relies on some programming commands to generate the global optimal result. The regression Eqs. (1)–(3) developed by RSM approach for groove width, heat affected zone thickness and groove depth are utilized in generation of objective function for PSO. The minimum and maximum values of the process parameters were used as constraints for the objective function. For multiple response optimizations using PSO, the following equation is proposed by taking into consideration of all the responses simultaneously optimized and optimum parameter settings can be considered by the objective function:

$$Z_{\text{GLOBALMIN}} = W_1 * \frac{Y_{\text{GWD}}}{Y_{\text{GWDMIN}}} + W_2 * \frac{Y_{\text{HAZ}}}{Y_{\text{HAZMIN}}} + W_3 * \frac{Y_{\text{GD}}}{Y_{\text{GDMIN}}} \quad (4)$$

Figure 3 presents the convergence plot, which aims to optimize the abovementioned three laser microgrooving responses in the presence of PSO specific parameters. Here, the initial swarm size is set at 50 with maximum number of iteration of 100. The constants  $C1$  and  $C2$  are taken as 2. By solving the optimization problem with PSO, it was found that the  $Z_{\text{MIN}}$  value is 0.2949, occurring at a weightage of 0.80 ( $W_1$ ) to upper width. Also 10% i.e. weightage of 0.1 ( $W_1$  and  $W_3$ ) equal importance has been given to other two responses (heat affected zone thickness and groove

**Table 3** Results of ANOVA for response model

Regression	Groove width (GWD)			HAZ			Groove depth (GD)					
	<i>F</i>	<i>P</i>	<i>R</i> <sup>2</sup>	<i>R</i> <sup>2</sup> (adj)	<i>F</i>	<i>P</i>	<i>R</i> <sup>2</sup>	<i>R</i> <sup>2</sup> (adj)	<i>F</i>	<i>P</i>	<i>R</i> <sup>2</sup>	<i>R</i> <sup>2</sup> (adj)
	27.14	0.000	95.96%	92.42%	25.15	0.000	95.65%	91.85%	31.05	0.000	96.45%	93.34%



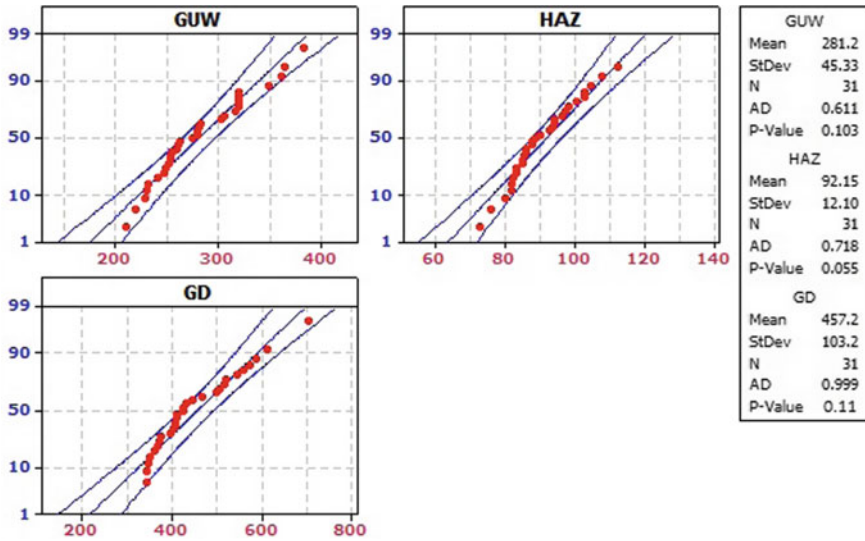


Fig. 2 Normal probability plot for technological response characteristics of laser microgroove

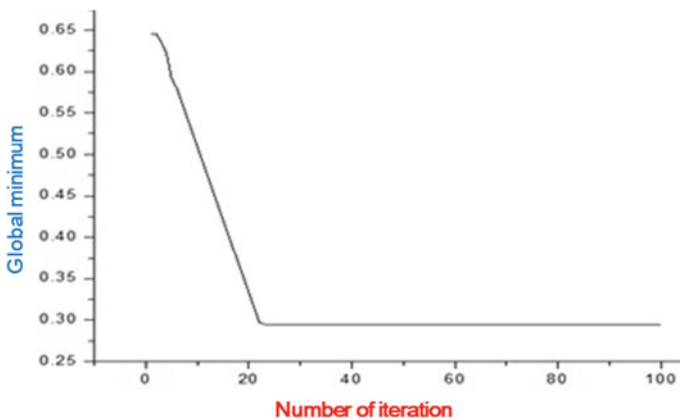
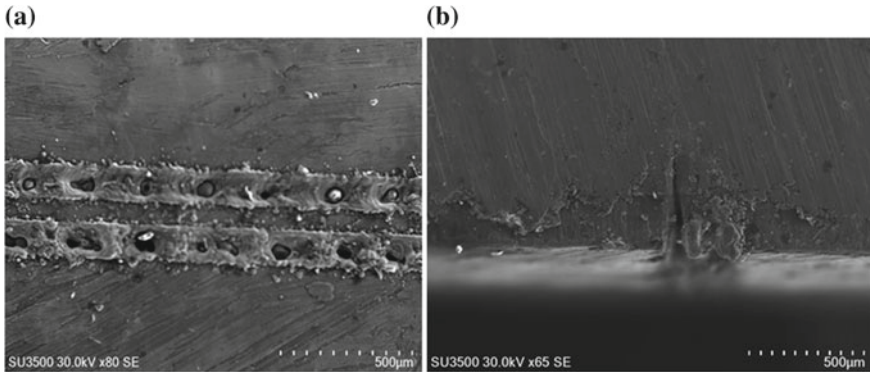


Fig. 3 Optimal convergence curve for multi-objective PSO

depth). Moreover, it can be concluded that the optimal solution occurs at sudden decrease in global minimum with a less processing time due to lesser complexity as well as significant improvement in computational efficiency of PSO algorithm. The optimal process parameters setting for microgrooving variables in laser machining of titanium alloy ( $Ti_6Al_4V$ ) are diode current 18.5 amp, pulse frequency 40 kHz, scan speed 40 mm/s, no. of passes 13, with estimated groove width (GWD) of 0.124 mm, heat affected zone (HAZ) of 0.123 mm and groove depth (GD) of 0.232 mm. Finally, an additional experiment is performed with the optimal configuration (suggested by



**Fig. 4** SEM micrograph showing machined surface under optimum cutting conditions

PSO) in order to observe the machined microgroove using scanning electron microscope (SEM), shown in Fig. 4.

## 4 Conclusions

In the present work, laser engraving has been carried out on  $Ti_6Al_4V$  substrate using argon gas. The experiments were modeled using CCD based RSM approach. Empirical models proposed for the technological response characteristics such as, groove upper width as well as depth and heat-affected zone have  $R$ -square value close to one and  $P$ -value less than 0.05, which ensured the greater statistical significance with excellence of fit for the model. The normal probability plot ensures that the residuals distributed fairly near to a straight line showing the normality dispersion of errors as well as implying the sources associated with the models are significant. Anderson–Darling test for model show adequate, as  $P$ -value is over 0.05 at 95% confidence level. The regression equations developed in RSM approach were used to generate the objective function for the PSO approach, which demonstrated the ability to optimize and to accurately model the technological response characteristics of microgroove through advances in computer technology. By solving the optimization problem with PSO, corresponds to optimal setting of process parameters (diode current = 18.5 amp, pulse frequency = 40 kHz, scan speed = 40 mm/s, number of passes = 13) with estimated upper width 0.124 mm, heat affected zone 0.123 mm and depth 0.232 mm. The suggested multiple approaches (experimental, statistical, and computational) are reliable methodologies for improving laser microgrooving process and can be used in model predictive control, real-time process monitoring, and optimization in different machining process.

## References

1. Dhupal D, Doloi B, Bhattacharyya B (2009) Modeling and optimization on Nd:YAG laser turned micro-grooving of cylindrical ceramic material. *Opt Lasers Eng* 47:917–925
2. Kibria G, Doloi B, Bhattacharyya B (2013) Predictive model and process parameters optimization of Nd:YAG laser micro-turning of ceramics. *Int J Adv Manuf Technol* 65:213–229
3. Biswas R, Kuar AS, Biswas SK, Mitra S (2010) Artificial neural network modelling of Nd:YAG laser microdrilling on titanium nitride—alumina composite. *J Eng Manuf* 224:473–482
4. Kibria G, Doloi B, Bhattacharyya B (2014) Modelling and optimization of Nd: YAG laser micro-turning process during machining of aluminum oxide ( $Al_2O_3$ ) ceramics using response surface methodology and artificial neural network. *Manuf Rev* 1:1–8
5. Kuar AS, Acherjee B, Ganguly D, Mitra S (2012) Optimization of Nd:YAG laser parameters for microdrilling of alumina with multiquality characteristics via Grey-Taguchi method. *Mater Manuf Processes* 27:329–336
6. Kibria G, Doloi B, Bhattacharyya B (2012) Optimisation of Nd: YAG laser micro-turning process using response surface methodology. *Int J Precis Technol* 3:14–36
7. Biswas R, Kuar AS, Mitra S (2015) Process optimization in Nd:YAG laser microdrilling of alumina–aluminium interpenetrating phase composite. *J Mater Res Technol* 4:323–332
8. Nandi S, Kuar AS (2015) Parametric optimisation of Nd:YAG laser micro-drilling of alumina using NSGA II. *Int J Mach Mach Mater* 17:1–21
9. Mohammed MK, Umer U, Al-Ahmari A (2017) Optimization of laser micro milling of alumina ceramic using radial basis functions and MOGA-II. *Int J Adv Manuf Technol* 91:2017–2029
10. Kalita K, Shivakoti I, Ghadai RK (2017) Optimizing process parameters for laser beam micro-marking using genetic algorithm and particle swarm optimization. *Mater Manuf Process* 32:1101–1108
11. Dhupal D, Mohanty S, Dixit SR, Das SR, Nanda BK (2018) Micromachining on Al-SiC based metal matrix composite using DPSS laser. *Mater Today: Proc* 5:11304–11318